ISSN 1995-0780, Nanotechnologies in Russia, 2017, Vol. 12, Nos. 1–2, pp. 73–85. © Pleiades Publishing, Ltd., 2017.
Original Russian Text © D.A. Gvozdev, E.G. Maksimov, M.G. Strakhovskaya, M.V. Ivanov, V.Z. Paschenko, A.B. Rubin, 2017, published in Rossiiskie Nanotekhnologii, 2017, Vol. 12, Nos. 1–2.

The Effect of Ionic Strength on Spectral Properties of Quantum Dots and Aluminum Phthalocyanine Complexes

D. A. Gvozdev[a]*, E. G. Maksimov[a], M. G. Strakhovskaya[a,b], M. V. Ivanov[a], V. Z. Paschenko[a], and A. B. Rubin[a]

[a] *Department of Biology, Moscow State University, Moscow, 119234 Russia*
[b] *Federal Research and Clinical Center of Specialized Types of Health Care and Medical Technologies, Federal Biomedical Agency of Russia, Moscow, 115682 Russia*
**e-mail: danil131054@mail.ru*

Received July 1, 2016; in final form, October 13, 2016

Abstract—The effect of ionic strength on spectral properties of negatively charged semiconductor (CdSe/ZnS) nanocrystals (quantum dots, QDs) and polycationic aluminum phthalocyanines (PCs) is considered. A QD/PC complex, formed via self-assembly, remains stable throughout a wide range of ionic strength values of a solution and [PC]/[QD] concentration ratio. The efficiency of nonradiative energy transfer from QDs to PCs rises with an increase in the ionic strength of solution. The fluorescence amplification factor of PC reduces with an increase in number of PC molecules in a complex with a quantum dot, reaching negative values at high [PC]/[QD] ratios. This is probably due to the decrease in the effect of energy migration on the total PC fluorescence upon its own significant absorption ability of a large number of acceptors. These effects are of interest to develop selection principles of components for hybrid complexes stabilized with electrostatic interaction.

DOI: 10.1134/S1995078017010050

INTRODUCTION

Phthalocyanines (PCs) constitute the largest group of macrocyclic dyes and are assigned to tetrabenzoazaporphyrines by their chemical structure. PCs possess high photostability and, being in a photoexcited state, start photosensitized reactions involving reactive oxygen species, including singlet oxygen [1]. The latter forms as a result of energy migration from a triplet excited state of PC to a triplet ground one of a molecular oxygen. Fluorescent and sensitizing properties of PCs are used in biomedical applications for fluorescence imaging and diagnosis [2], antitumor photodynamic therapy (PDT) [3], the photodynamic inactivation of microorganisms [4], and to change intracellular distribution of administered compounds [5].

There are several ways to optimize the physicochemical and spectral properties of PCs. Including diamagnetics such as Zn^{2+} or Al^{3+} into a macrocycle as a central metal ion rises the yield of triplet excited states of PCs [6]. The hydrophobic properties of a macrocycle of metal PCs contribute to the formation of nonfluorescent PC dimers, being unable to generate singlet oxygen in aqueous solutions. The formation of substituted metal PCs via introducing the ionic substituents onto the periphery of macrocycle, however, reduces the aggregation of PCs in water [7]. A promising direction is to create hybrid complexes of PC fluorescent labels and photosensitizers with molecules and nanoparticles that reinforce the photodynamic properties of photosensitizers owing to modifying their spectral properties and targeted delivery of the hybrid structure into a cell or its compartments [8, 9], for example, with fullerenes [10] or quantum dots (QDs) [11–15].

QDs have long attracted attention for using in PDT and fluorescent diagnostics [16–18]. Although QDs do not possess their own significant photodynamic properties, they can be used as a fluorescent label to visualize tumors owing to the high quantum yields of fluorescence [19]. QDs can also be considered a base to develop multicomponent complexes with antibodies or peptides that raise the efficiency of penetration of a complex into a cell [20, 21]. A more interesting fact is that QDs can be used to modify the spectral properties of photosensitizers. QDs can act as artificial "light harvesters," or antennas, capable of transmitting the energy to acceptors of different nature according to the inductive resonance mechanism (FRET) [22, 23]. PCs have strong absorption in the far-red or infrared regions of a spectrum with extinction coefficients more than 10^5 M^{-1} cm^{-1} [7, 24], but the absorption of PCs, by contrast, is small in the visible region of the spectrum (400–600 nm). The effective absorption cross section for PCs, especially in the blue-green

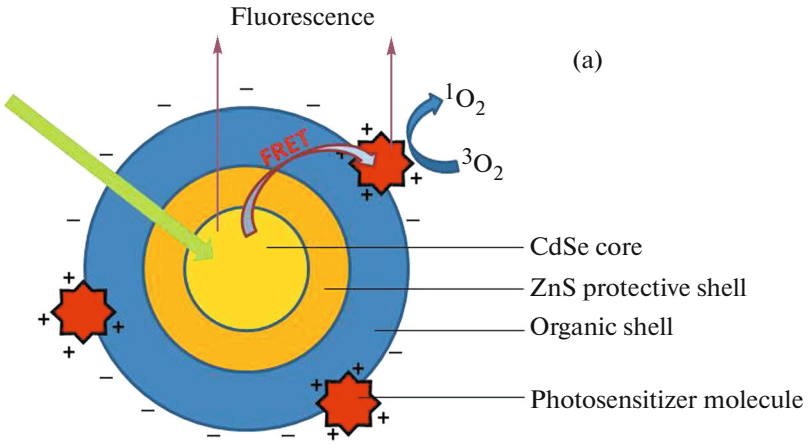

(b)

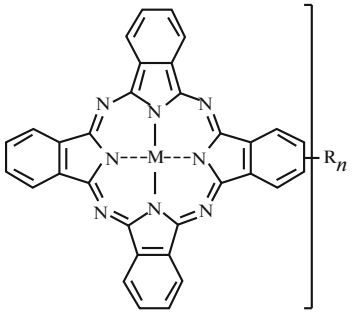

$R = HOCH_2CH_2-\overset{\overset{CH_3}{|}}{\underset{\underset{CH_3}{|}}{N^+}}-CH_2^-$ Cl^-

M: AlCl

$n = 4\text{-}5$ PC(+4.5)

$n = 6\text{-}7$ PC(+6.5)

(c)

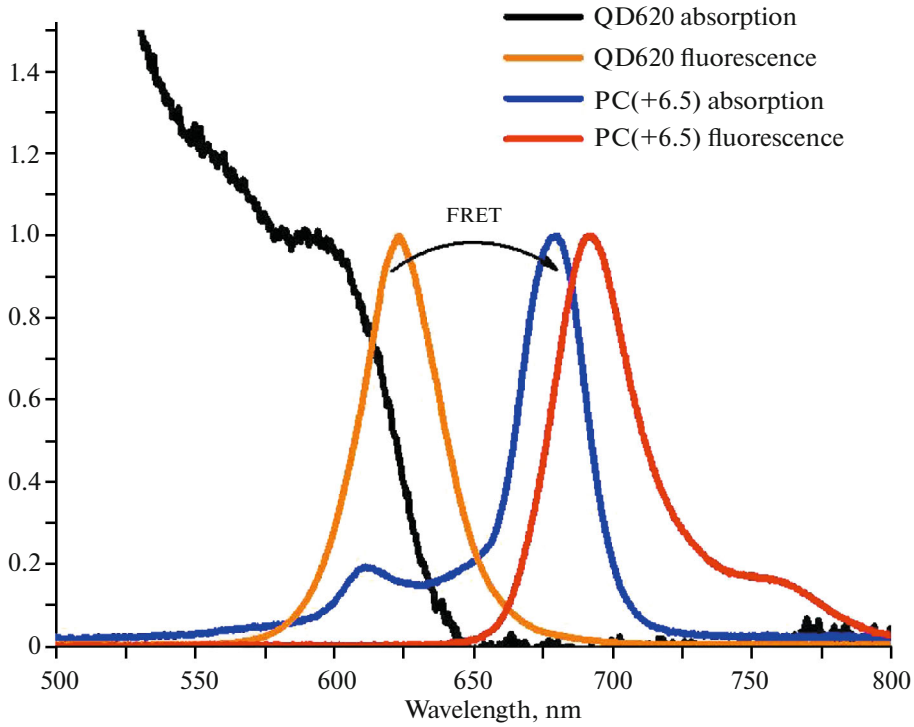

Fig. 1. (Color online) (a) Scheme of QD/PC hybrid complex; (b) structural formulas of PCs, where *n* is average degree of inclusion of substituents R; and (c) normalized absorption and fluorescence spectra of QD620 and PC(+6.5).

Table 1. Spectral properties of semiconductor nanocrystals

Type of QD	Emission maximum, nm	Fluorescence quantum yield, %	Diameter of QD core, nm	Molar extinction coefficient, M^{-1} cm^{-1}
QD600	613	4.5	3.3	141400
QD620	622	38.4	4.1	240150

part of the spectrum, rises because of the QD/PC complex formation (Fig. 1a) and energy migration from QDs to PCs. As a result, the intensity of PC fluorescence and generation of reactive oxygen species rise [11, 12]. Such complexes may be useful in the PDT of surface tumors and, probably, in the two-photon PDT of tumors of deep layers, where the intrinsic absorption of PCs is insufficient even in the red region of the spectrum.

The applicability of this kind of technology in vivo, however, depends strongly on the properties of internal environment of an organism, which is not the same as a solution in pure water. Ionic strength of the medium is an important parameter that can have a significant impact on the photodynamic properties and stability of the QD/PC complexes. At present, most of the QD/PC hybrid complexes investigated were obtained via self-assembly and stabilization through electrostatic interactions. Thus, the crucial important question is preserving the photodynamic properties of such complexes upon the ionic strength of the environment, corresponding to those in vivo [15].

In this work we examine the stability of QD/PC hybrid complexes stabilized electrostatically upon a change in the ionic strength of the solution in its physiological values. The structural stability of the complex was studied in solutions with increasing ionic strength. The change in the spectral characteristics of components of the complex depending on the ionic strength of the environment was especially studied because the efficiency of energy transfer by the FRET mechanism depends on the overlap of the fluorescence spectrum of an energy donor (QD) with that of its acceptor (PC) and a distance between the QD and PC in the complex.

EXPERIMENTAL

Two polycationic cholinyl-substituted aluminum PCs (Fig. 1b), having an average degree of substitution, 4.5 and 6.5, (PC(+4.5) and PC(+6.5)) synthesized in the NIOPIK State Research Center, Russia were used. The coefficients of molar extinction, as well as absorption and fluorescence maxima of these compounds in aqueous solution, are presented in Table 2.

The QDs having CdSe as a core, produced by the Nanotech-Dubna Company (Russia), were used as an energy donor to increase the effective absorption cross section of PCs. The ZnS protective shell passivates the surface defects of the crystal lattice of a nucleus, which increases the fluorescence properties of QDs, whereas the outer shell of organic ligands (carboxyl groups oriented to the outside environment) provides water solubility and the negative charge of QDs. PC(+4.5), PC(+6.5), and QDs of this type formed hybrid complexes with highly efficient energy transfer in accordance with the results of our previous work [25]. QD600 and QD620 were selected in this work because their fluorescence quantum yields differ by more than eightfold. The characteristics for QD600 and QD620 are listed in Table 1. The diameters of QD cores, their molar extinction coefficients, and their concentrations were calculated with the empirical formulas pro-

Table 2. Spectral properties of substituted aluminum PCs in solutions with different ionic strengths. Fluorescence excitation wavelength is 655 nm

	Ionic strength of solution, M	Position of absorption peak, nm	Position of fluorescence maximum, nm	Molar extinction coefficient, M^{-1} cm^{-1}	Fluorescence intensity, a. u.	Fluorescence lifetime, ns
PC(+4.5)	0	681.8	697.1	150.000*	181.3	5.35
	0.05	683	698.5	164.200	243.9	5.37
	0.1	683.4	698.7	171.000	251.5	5.36
	0.15	683.7	698.7	175.900	251.9	5.34
	0.2	683.7	698.7	178.200	242.6	5.32
PC(+6.5)	0	679.8	693.6	185.000*	217.5	5.04
	0.05	681.4	694.8	190.800	301.9	5.05
	0.1	682.4	694.8	195.800	303.9	5.06
	0.15	682.7	694.8	200.000	301.2	5.05
	0.2	683	694.8	206.000	307.9	5.05

*Molar extinction coefficients in an aqueous solution (without added salts) are given in accordance with the data by Makarov et al. [7].

vided by Yu et al. [26]. The fluorescence quantum yield of QDs was determined with the formula

$$\varphi = \varphi_0 \frac{S}{S_0}\frac{D_0}{D}, \quad (1)$$

where φ is the relative quantum yield, S is the area under the fluorescence spectrum, and D is the optical density of the solution at the fluorescence excitation wavelength—455 nm. Index 0 corresponds to fluorophore-standard with a known fluorescence quantum yield φ_0. A rhodamine B was used as a standard; fluorescence quantum yield was taken to be 0.65 in an alcoholic solution [27]).

Distilled water was used as a solvent in the experiments. To assess the effect of ionic strength on the electrostatic interaction of QDs and PCs in a complex, solutions with different ionic strengths (0, 0.05, 0.1, 0.15 and 0.2 M) were prepared; the ionic strength of human plasma and other biological fluids is close to 0.15. The required ionic strength value was achieved by adding the 2-M NaCl solution to the QD/PC one.

Absorption spectra were acquired on a CCD USB2000 spectrometer equipped a deuterium-tungsten lamp DT-MINI-2-GS (Ocean Optics, United States) as a light source. A CCD USB4000 spectrometer (Ocean Optics, United States) was used to record stationary fluorescence spectra. The measurements were performed in 10 × 2 mm fine quartz cells. Absorption of PC at a fluorescence excitation wavelength of QDs due to shielding reduces the real intensity of an excitation light beam. In addition, the absorption of PCs at fluorescence wavelengths of QDs reduces the measured luminescence intensity of QDs. Thus, the measured fluorescence intensity of QDs becomes less than the true one. To assess and for leveling of these effects, a correction coefficient proposed earlier was used [28]:

$$\eta = \frac{A_{xo}A_{yo}(1-10^{-A_{xi}})(1-10^{-A_{yi}})}{A_{xi}A_{yi}(1-10^{-A_{xo}})(1-10^{-A_{yo}})}, \quad (2)$$

where A_{yo} and A_{xo} are the absorption of energy donor (QDs) at the wavelength of fluorescence maximum of QDs and fluorescence excitation of QDs (405 nm), respectively, whereas A_{yi} and A_{xi} are absorbance of a donor and acceptor mixture at the same wavelengths. The efficiency of migration energy $W = 1 - I_{DA}/\eta I_D$ was calculated with a coefficient, where I_{DA} is fluorescence intensity of energy donor (QDs) in the presence of an acceptor (PC) and I_D is the fluorescence intensity of QDs in the control without quencher.

To study the dynamics of photo-induced changes in fluorescence and optical density, a Spectrasuite software (Ocean Optics, United States) was used. The instantaneous fluorescence spectra with picosecond time resolution were acquired on a measurement complex based on a SimpleTau140 single-photon counting system (Becker & Hickl, Germany) [29]. To excite fluorescence of QDs and PCs, LDH-405 and PLS-445/660 light-emitting diode lasers were used (InTop, Russia): pulse duration was 25 ps; pulse repetition frequency was 10 MHz; energy of a single pulse was 13 pJ; and fluorescence excitation wavelengths were 405, 445, and 655 nm, respectively. The fluorescence signal through an optical fiber at an angle of 90° towards exciting light was directed to a MS 125 polychromator (Becker & Hickl, Germany). Then fluorescence was recorded in a photon counting mode on a PML-16-1-C 16-channel detector (Becker & Hickl, Germany) at the range of 530–730 nm with a diffraction grating having a resolution of 12.5 nm/channel. Mean fluorescence lifetime was calculated with a formula

$$\tau = \sum_i a_i \tau_i, \quad (3)$$

where τ_i is lifetime of the ith component and a_i is a normalized contribution of the ith component ($\sum a_i = 1$). The kinetics of fluorescence decay was approximated with a sum of three exponents for QDs and one for PCs.

To study molecular rotation rate, kinetics of fluorescence polarization was recorded. To perform this, the fluorescence decay kinetics was registered at the two positions of WP25M-UB broadband polarization filters (Thorlabs, United States) placed in front of a cuvette with a sample and on a channel registration of fluorescence signal of the sample. The kinetics of the fluorescence anisotropy $r(t)$ was calculated with the formula

$$r(t) = \frac{I_{VV}(t) - I_{VH}(t)}{I_{VV}(t) + 2I_{VH}(t)} \quad (4)$$

where $I_{VV}(t)$ and $I_{VH}(t)$ are fluorescence decay kinetics in parallel and crossed polarizers, respectively. The measurements were performed in a thermostated cell Qpod 2e (Quantum Northwest, United States) at 25°C. The kinetics of fluorescence anisotropy was approximated via the sum of the exponents $r(t) = \sum_i^n r_{0i} e^{-t/\theta_i}$, where r_{0i} is the maximum (fundamental) anisotropy of the ith component and θ_i is correlation rotation time of the ith component ($n = 1, 2$).

All calculations were performed with OriginPro 9.1 (OriginLab Corporation, United States) and SPCImage (Becker & Hickl, Germany) packages. Each experiment was repeated at least 3 times.

RESULTS AND DISCUSSION

Influence of Ionic Strength on Spectral Characteristics of PCs

The ionic strength of a solution and the qualitative composition of ions have a significant impact on spectral characteristics and photodynamic of porphyrins

and PCs; in some cases, it leads to the formation of dimers and aggregates [30, 31]. The dimers are easily detected with a peak at 630–640 nm in the absorption spectrum. We found no aggregation of PC molecules in the selected range of ionic strength values (0.05–0.2 M) of the PC solutions used. Nevertheless, the addition of a salt to PC water solutions causes a change in the absorption and fluorescence spectra (Table 2).

When the ionic strength of the solution rises, we observed an increase in molar extinction coefficient of PCs, as well as a shift in their absorption and fluorescence spectra towards longer wavelengths, accompanied by a decrease in the Stokes shift. This is probably a consequence of a change in the solvation state of the PC molecule and shielding of the charged side groups of PC by counterions, because a change in state and position of peripheral substituents at different ionic strength values affects the optical properties of PCs [11]. When a salt was added (increasing the ionic strength value up to 0.05 M), we also observed an increase in fluorescence intensity of PCs. A further increase in ionic strength up to 0.2 M, however, had no significant effect. The formation of a shell of counterions around PC molecules upon the initial increase in ionic strength of the solution up to 0.05 M has apparently the highest impact in the observed effect [30, 31]. Although an increase in ionic strength and optical density of the PC solution was observed (Table 2), no relation $I/I_0 = D/D_0$ was reached, where I and D are fluorescence intensity of PC and optical density of its solution with a nonzero ionic strength, whereas I_0 and D_0 are the same parameters at zero ionic strength, respectively. As a result, the fluorescence quantum yield of PC rises in the presence of the salt. At the same time, we did not observe reliable changes in the fluorescence lifetime of PCs depending on the ionic strength; in other words, the sum of deactivation constants of the PC excited state must remain unchanged. This may indicate that an increase in ionic strength causes a change in the charge state of PC molecule and, as a result, an increase in fluorescence constants and, simultaneously, a decrease in the probability of deactivation of the excited state by the other channels–internal conversion or singlet–triplet transition.

Influence of Ionic Strength on Spectral Characteristics of QDs

After the absorption of a quantum of light in QD and formation of exciton, one of the charge carriers (electrons or "hole") can be located on crystalline structure defects of QD. Thus, the QD is in the "off" state, when the recombination of an electron–hole pair and, therefore, fluorescence are impossible. Although the mechanisms of charge carrier capture by nanocrystal defects are debated [32], the conformational state of ligands in an outer organic shell QDs is assumed to have an effect on the probability of transition of QD into off state. When the ionic strength of the solution increased, QDs exhibited a significant decrease in intensity (Fig. 2) and fluorescence lifetime: QD600, from 11.7 ns in the aqueous solution to 9.8 ns in a solution with 0.2 M in ionic strength, and QD620, from 19.4 to 16.7 ns. The sodium cations, forming a counterion shell on a negatively charged QD surface, possibly change the local electric field and charge state of the QD organic shell so that it raises the probability of localization of a charge carrier on nanocrystal defects and, thereby, reduces fluorescence quantum yield. It should be noted that fluorescence of QD600 is quenched more strongly than that of QD620 upon a fixed value of the ionic strength. The probability of transition of QD into the off state depends largely on the protective shell thickness and the number of defects on QD crystal lattice [33] and determines the fluorescence quantum yield of QDs. In this range of ionic strength values (Fig. 2), the fluorescence of QD600 is quenched more strongly than that of QD620 probably because of the ZnS thin protective shell of this QD (see the Section *Influence of Ionic Strength on Efficiency of Energy Transfer in QD/PC Hybrid Complex*').

Influence of Ionic Strength on Electrostatic Binding of QDs and Aluminum PCs

A convenient way to test the efficiency of complexation is to analyze the kinetics of fluorescence anisotropy of PC molecules, whose rotation rate depends on weight, size, and shape of the hydrated PC or its complex with QDs. In this case, we used a red laser with 655 nm in wavelength to excite fluorescence, because such excitation is selective for PCs (Fig. 1c). When the sources with shorter wavelength are used, the recorded anisotropy can be additionally reduced because of the energy transfer from QDs to PCs [34].

In the PC control aqueous solution and in absence of QD, both types of PC exhibited two-component anisotropy kinetics with the characteristic correlation rotation time values, 0.1 and 0.5–0.6 ns (Fig. 3, blue curve); $r_0 = \sum r_{0i}$ did not exceed 0.1, which is the upper limit of fundamental anisotropy for the molecules of this type [35]. Considering that the absorption dipole moments (in the two Q-bands, where fluorescence excitation happened) of PCs lie in the macrocycle plane [36], the fast component corresponds to a rotation in the macrocycle plane. This results in a significant decrease in amplitude anisotropy from 0.09 to 0.02. The slow component with a smaller amplitude (about 0.02) corresponds to out-of-plane rotation of the macrocycle, and this requires more restructuring of the water environment of PC molecule. It is interesting that when a salt is added to such a solution, kinetics of anisotropy becomes one-component with a characteristic rotation time to be 0.4 ns. This probably suggests that the shell of counterions around the PC molecule contributes to changing the shape of the

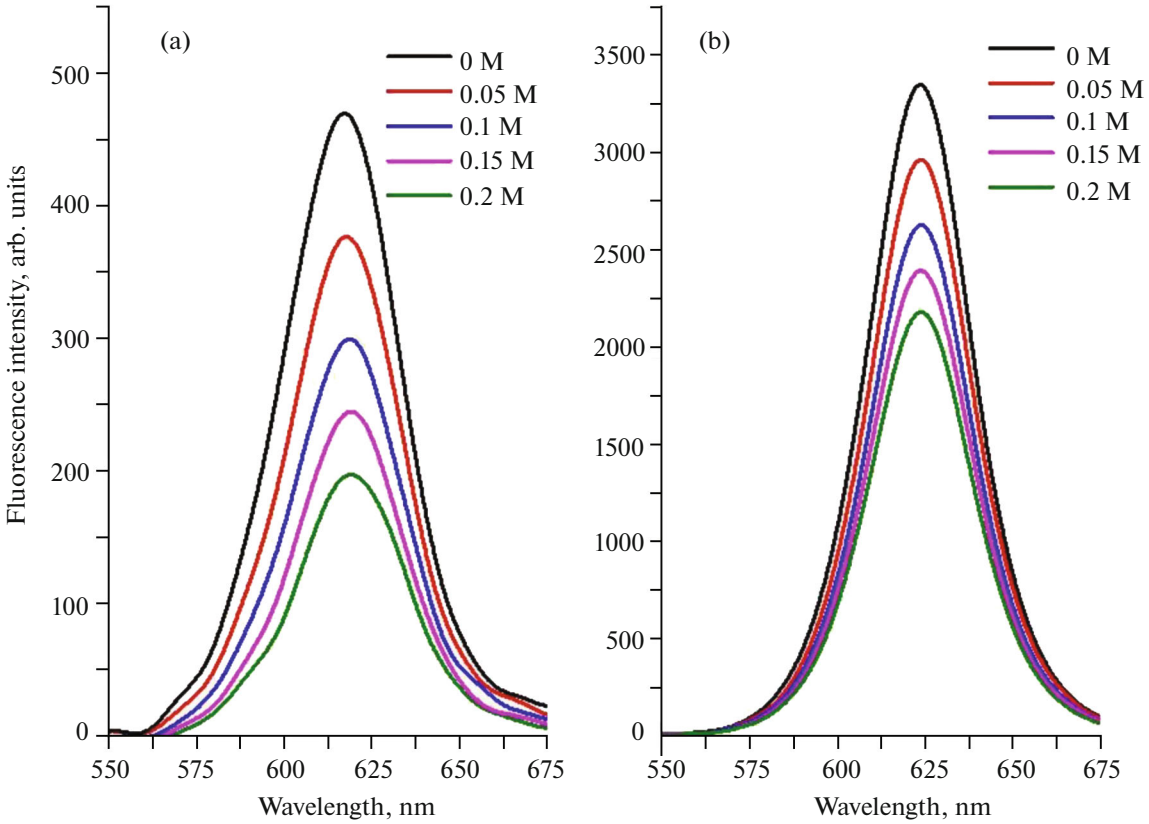

Fig. 2. (Color online) Changes in fluorescence spectrum of 0.1 μM solution of (a) QD600 and (b) QD620, depending on ionic strength of solution.

molecule rotating together with a hydration shell from disc-shaped to nearly spherical; this causes the degeneration of the correlation times of different rotation axes to form one.

When an equimolar amount of QDs is added to the PC solution, anisotropy kinetics involves a new component with characteristic values of the correlation lifetimes, 2.8–3 ns in aqueous solution and 2.5 ns in that with 0.2 M in ionic strength. This time corresponds apparently to the rotation of the PC/QD complex. The fast component, being characteristic for free PCs, is observed in the PC/QD solution (Fig. 3) only in the first few minutes after preparation of the solution. Kinetics of anisotropy for PC/QD solutions, incubated for half an hour, contain only one component corresponding to the rotation of PC/QD complex (Fig. 6b). Thus, by this time, all the PC molecules, being in the solution, are bound with QDs. The monoexponential character of anisotropy kinetics, reached after incubation of PC with QDs, indicates that PC molecules do not undergo any rotational motions on the QD surface.

Thus, most of the PC molecules are bound with the QD surface in the entire range of concentrations and ionic strength values.

Influence of Ionic Strength on Efficiency of Energy Transfer in QD/PC Hybrid Complex

The efficiency of energy migration in the complex is determined by the degree of fluorescence quenching of energy donor; in our case, it was QD. To study the efficiency of energy migration in the QD/PC complex depending on the ionic strength, five solutions, having various ionic strength values (0, 0.05, 0.1, 0.15, and 0.2 M), were prepared. Then the sequential addition of a quencher (PC) to these solutions, containing 0.2 μM of QD, was performed, so that each new portion of PC increased its concentration by 0.2 μM in the final solution. Thus, the [PC]/[QD] ratio in the solution increased from 1 : 1 to 10 : 1. When 3 min passed after the addition of each next portion of PC and equilibrium has been reached, the intensity and fluorescence lifetime of a donor and acceptor of energy were recorded with photon counting. At the same time, the stationary fluorescence spectra were acquired, so that it allowed controlling a possible change in shape of the spectra. $I_{DA}/\eta I_D$ and τ_{DA}/τ_D ratios were constructed depending on PC concentration on the basis of these data, where I_{DA} and τ_{DA} are the intensity and lifetime of fluorescence of energy donor (QDs), respectively, in the presence of an acceptor (PCs), whereas I_D and τ_D are intensity and

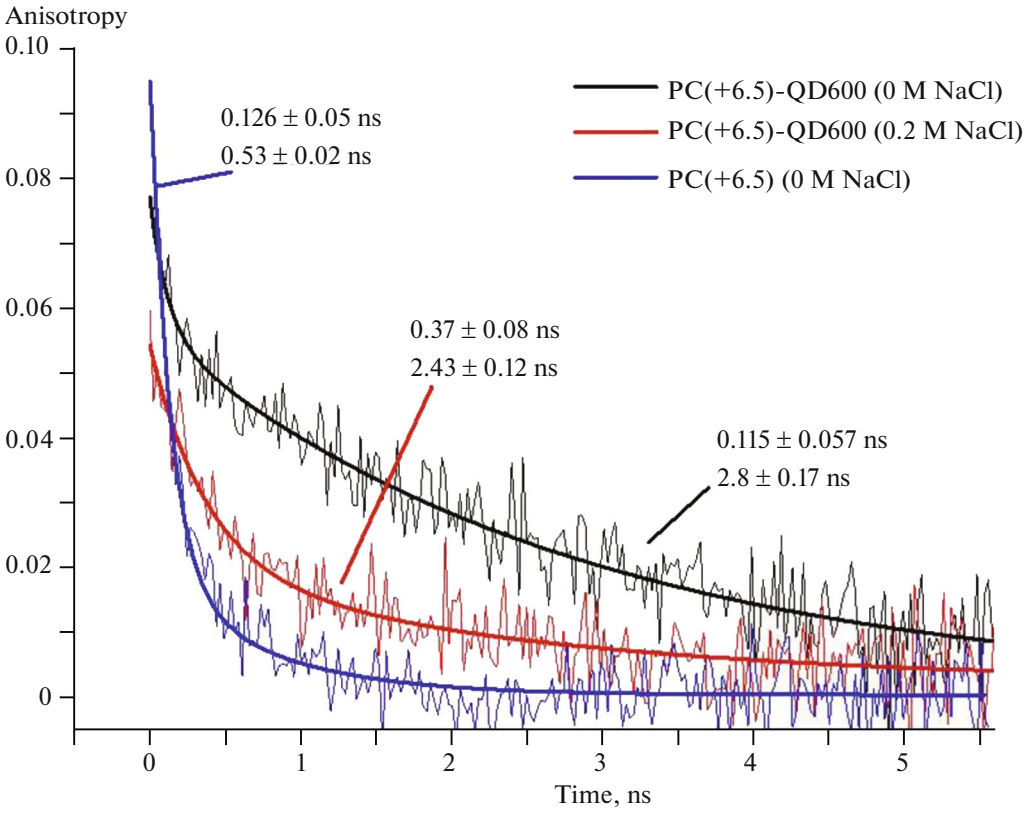

Fig. 3. (Color online) Kinetics of fluorescence anisotropy of PC(+6.5) in an aqueous solution (blue curve), in a complex with QD600 ([PC]/[QD] = 1 : 1) in an aqueous solution (black curve), and in a solution with ionic of 0.2 M (red curve).

lifetime of QD fluorescence, respectively, upon control in the absence of quencher. Fluorescence quenching data for QDs by aluminum PCs are shown in Fig. 4; QD600 was used as an example. It should be noted that the ratios $I_{DA}/\eta I_D$ and τ_{DA}/τ_D are almost identical for each QD/PC pair and ionic strength value, indicating that there is no significant contribution to the static quenching.

The energy migration efficiency $W = 1 - \tau_{DA}/\tau_D$ can be easily calculated if relation τ_{DA}/τ_D is known. In addition, the overlap integrals of fluorescence spectra of QDs (S) and absorption spectra of PCs were calculated with PhotochemCAD sotware, so it was possible to determine Forster radii $R_o = \sqrt[6]{8.8\times10^{-25}(\chi^2 n^{-4}\varphi_d S)}$ for each complex, where φ_d is fluorescence quantum yield of energy donor in the absence of an acceptor, χ^2 is a factor that describes the relative orientation of dipole moments of donor and acceptor (χ^2 is accepted to be 2/3 in the solution because of random orientation of dipole moments), and n is a refractive index of the medium. The distance R between the donor and acceptor is determined with the formula $W = 1/(1 + (R_o/R)^6)$, whereas the constant rate of energy migration is calculated as follows: $k = (R_0/R)^6/\tau_D$. The above parameters are shown in Table 3; they are given for all QD/PC pairs in aqueous solution with the concentration ratio of [PC]/[QD] = 1 : 1.

Table 3 shows that the distance R between the donor and acceptor for each QD is practically independent from the PC type. This suggests that PC molecules form stable complexes with QDs in aqueous solutions, and the distance R may be apparently considered as a QD radius. Thus, the data from Table 3

Table 3. FRET parameters for various combinations of QDs and PCs: R_o, Forster radius; R, distance between donor and acceptor of energy; W, efficiency of energy migration; S, overlap integral of fluorescence spectra of QDs and absorption of PCs; and k, rate constant of energy migration. Values are given for the complex with ratio of [PC]/[QD] = 1 : 1 in distilled water

Composition of complex		R_o, Å	R, Å	W, %	S, $\times10^{-13}$ cm^{-6}	k, $\times10^7$ s^{-1}
QD600	PC(+4.5)	29.8	42.1	11.1	3.33	1.46
	PC(+6.5)	33	40.8	21.9	6.15	3.27
QD620	PC(+4.5)	43.6	56.6	17.3	3.52	1.19
	PC(+6.5)	48.5	58	25.5	6.67	1.95

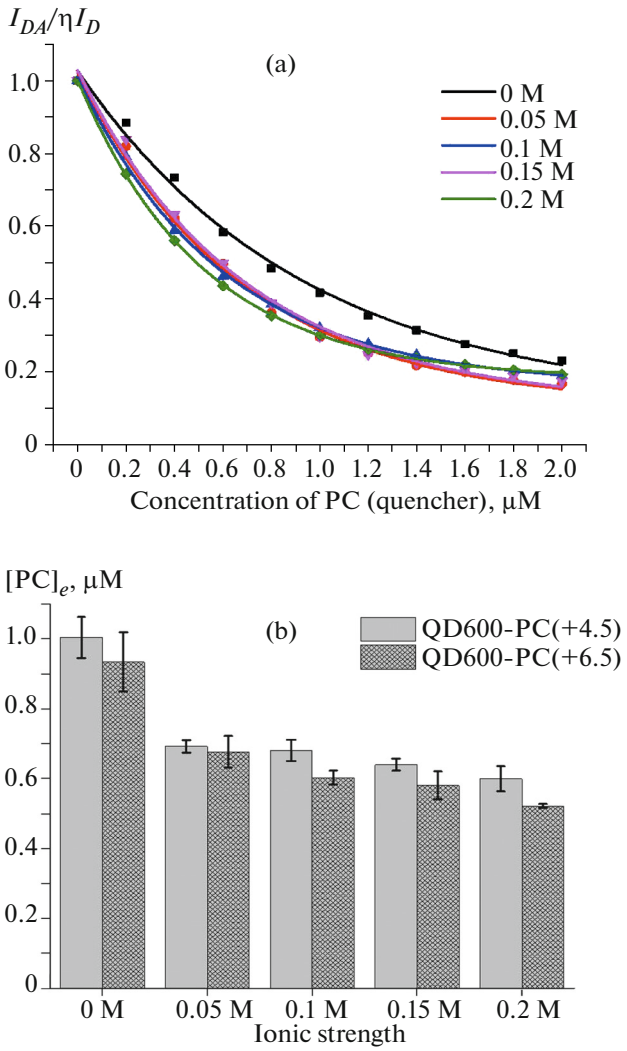

Fig. 4. (Color online) (a) Changes in relative fluorescence quantum yield of QD600 with PC(+6.5) depending on PC concentration upon different ionic strength and (b) PC concentration that causes fluorescence quenching of QDs by e times. It was obtained via approximation of fluorescence quenching curves of QDs on Fig. 4a by a monoexponent depending on ionic strength.

indicate the difference R for QD600 and QD620 can be estimated to be 1.6 nm taking into account an error, which is four times greater than the difference in the radii of their nuclei (Table 1). Considering that the composition and thickness of the organic shell, which provides water solubility and a charge for QDs, are similar for QD600 and QD620, the additional difference in radii of QDs, being 1.2 nm, should be associated with the nonuniform thickness of the ZnS protective shell of QD600 and QD620 nuclei. The shell of QD600 is probably very thin and, therefore, has low protection against charge carrier capture by the defects of nucleus crystal lattice [33]. This is consistent with the low fluorescence quantum yield of QD600 (4.5%).

Figure 4 shows that, upon transition from the aqueous solution into that with a nonzero ionic strength, the efficiency of energy migration from QDs to PCs increases, whereas a further increase in ionic strength values of the solution has little effect depending on its magnitude. We suppose that the observed pattern is a consequence of the combined effect of three different factors. Firstly, we observed an increase in the absorbing ability of PCs without QDs upon an increase in ionic strength (Table 2). An increase in the molar absorption coefficient of PCs leads to an increase in overlap integral value of the spectra (S) and, therefore, is largely responsible for increasing the efficiency of energy transfer upon a transition from aqueous solution to that with nonzero ionic strength. Secondly, a considerable decrease in fluorescence quantum yield of QDs occurs in the solution of QDs without PCs upon an increase in ionic strength and, on the contrary, it should cause a reduction in efficiency of energy migration in the system upon an increase in ionic strength of the solution. A third factor is a decrease in electrostatic forces between QDs and PCs in the complex upon an increase in ionic strength, which can reduce the efficiency of energy migration because of the increased distance between the donor and acceptor of energy. Analysis of data on fluorescence quenching of QDs, however, revealed no significant changes in the distance between QDs and PCs in the complex depending on the ionic strength value.

The fluorescence intensity of some photosensitizers rises because of energy migration from QDs, as was shown earlier [25, 37]; this is accompanied by an increase in generation rate of singlet oxygen. To assess the emission intensity of PCs in a complex with QDs, we calculated a fluorescence enhancement coefficient (A) with the following formula:

$$A = \frac{F - F_0}{F_0} = \frac{F}{F_0} - 1, \qquad (5)$$

where F is the fluorescence intensity of PCs in complex with QDs at an excitation wavelength of 405 nm and F_0 is the fluorescence intensity of PCs at the same concentration without QDs. A value A for PCs in pairs with different QDs ([PC]/[QD] = 1 : 1, for conformity to Table 3), depending on the ionic strength of the solution, is shown in Table 4.

Table 4 shows that the fluorescence enhancement coefficient for PCs with QD620 is more than those with QD600, which coincides with the greater efficiency of energy migration in PC/QD620 complexes. The greatest values of the parameter A, however, are observed in QD complexes with PC(+4.5) and not with PC(+6.5), although the efficiency of energy migration is smaller in QD complexes with PC(+4.5) than in those with PC(+6.5) (Table 3). It is important that the fluorescence enhancement coefficient does not reflect the efficiency of the most nonradiative energy transfer from QDs to the PCs. To directly

assess an increase in fluorescence intensity for PCs as a result of energy migration from QD, it is necessary to use the intensity I of PC fluorescence on a QD surface without energy migration as an F_0 parameter (in the formula (5)), because spectral properties of PC molecule can vary as a result of the adsorption of PC molecules on the surface of the QD outer organic shell. To verify this assumption, the fluorescence intensity of the PC solution was recorded before and after the addition of QD ([PC]/[QD] = 1 : 1) with the photon counting method at $\lambda = 655$ nm. Considering that the extinction coefficient of QDs is very small at the wavelength of the laser radiation (Fig. 1c), all the changes in PC fluorescence observed were not the result of energy migration. The results are shown in Fig. 5a.

Figure 5a (light grey columns) shows that PC fluorescence intensity reduces upon interacting with QDs ($I/F_0 < 1$), probably because of the change in PC conformation during adsorption on the QD surface. In the case of PC(+6.5), this decrease is quite significant—30% in a complex with QD600 and 45% in one with QD620. Considering that PC(+6.5) bears a larger number of charges than PC(+4.5), its electrostatic interaction with QDs must be stronger and thus have a more pronounced conformational change, which results in a greater decrease in fluorescence intensity. Thus, fluorescence intensity of PC on QD surface, but not in solution without QD, should be taken as a control in the formula for the fluorescence enhancement coefficient. In this case, the fluorescence enhancement coefficient of PC(+6.5) is higher than of PC(+4.5) because of energy migration (Fig. 5b).

In summary, we can make the following assumptions about the nature of interaction between QDs and PCs in the complex:

(1) QDs and PCs form a stable complex in an aqueous solution through electrostatic interaction between positively charged PC side radicals and negative charges of QD organic shell. We assume that the charges of the side radicals do not allow the PC molecule to penetrate into the organic shell.

(2) All side choline PC radicals participate during the interaction and formation of electrostatic bonds. Thus, the PC molecule is parallel to the QD surface and not able to rotate.

(3) A PC molecule bound with QD is in another conformational state than the equilibrium conformation in the solution, resulting in a decrease in PC fluorescence intensity.

We can make some comments relative to the impact of ionic strength upon an interaction between QDs and PCs in the hybrid complex on the basis of these assumptions. Firstly, an increase in ionic strength should cause a decrease in electrostatic interactions between QDs and PCs, so that conformations of free PC and that in complex with QDs will not be so different from each other. Secondly, the ionic strength value of the solution can directly influence the PC spectral properties bound with QDs. This means that the PC fluorescence intensity on the QD surface should rise and approach to its value in the PC solution without QDs upon an increase in ionic strength. Indeed, if we compare PC fluorescence intensity on the QD surface before and after the addition of sodium chloride to the solution, it appears that fluorescence intensity is higher in presence of NaCl by ~10% in all QD/PC pairs (data are not shown). Figure 5a, however, shows that the I/F_0 value is lower in presence of the salt (dark grey bars) than in water (light grey bars). This is probably due to the increase in PC fluorescence quantum yield in the presence of salt, so that the denominator of F_0 value for the solution with 0.2 M in ionic strength is significantly greater than that without the salt. A decrease in parameter A for PC (Table 4) is observed upon the addition of the salt for the same reason (increase in PC fluorescence intensity with increasing ionic strength in the control without QDs), whereas the efficiency in energy migration rises.

Table 4. Fluorescence enhancement coefficient of PCs in pairs with different QDs depending on ionic strength of solution

Ionic strength, M	QD600/ PC(+4.5)	QD620/ PC(+4.5)	QD600/ PC(+6.5)	QD620/ PC(+6.5)
0	1.32	4.36	0.81	2.26
0.05	0.63	3.44	–0.04	0.85
0.1	0.24	2.67	–0.19	0.69
0.15	0.01	2.02	–0.26	0.45
0.2	–0.04	1.81	–0.28	0.44

The 16-channel detector of photon counting with 200-nm spectral width enables one to simultaneously record fluorescence for both QDs and PCs, so the PC fluorescence enhancement coefficient was calculated simultaneously with the QD fluorescence quenching curves (Fig. 4a) for the same [PC]/[QD] ratios. This experiment showed a decrease in parameter A with an increase in PC concentrations. Some studies [38, 39] have shown that photodynamic and spectral properties of some photosensitizers in complexes with QDs upon high [PC]/[QD] ratios are less pronounced than the original PC solution. We may assume that if the total number of acceptors increases significantly on the QD surface, PC molecules, which fluoresce with reduced intensity compared to those in the solution and do not receive the energy from QDs, make a decisive contribution to sample fluorescence, so that PC fluorescence enhancement coefficient reduces and can become negative. Parameter A has been calculated for the PC(+4.5) in pairs with QD600 and QD620 in a large range of PC concentrations, where the [PC]/[QD] ratio was varied from 1 : 1 to 100 : 1 (Fig. 6a). Moreover, fluorescence anisotropy kinetics of PC(+4.5) (Fig. 6b) was calculated for the three points of this relationship ([PC]/[QD] = 25 : 1, 50 : 1, and

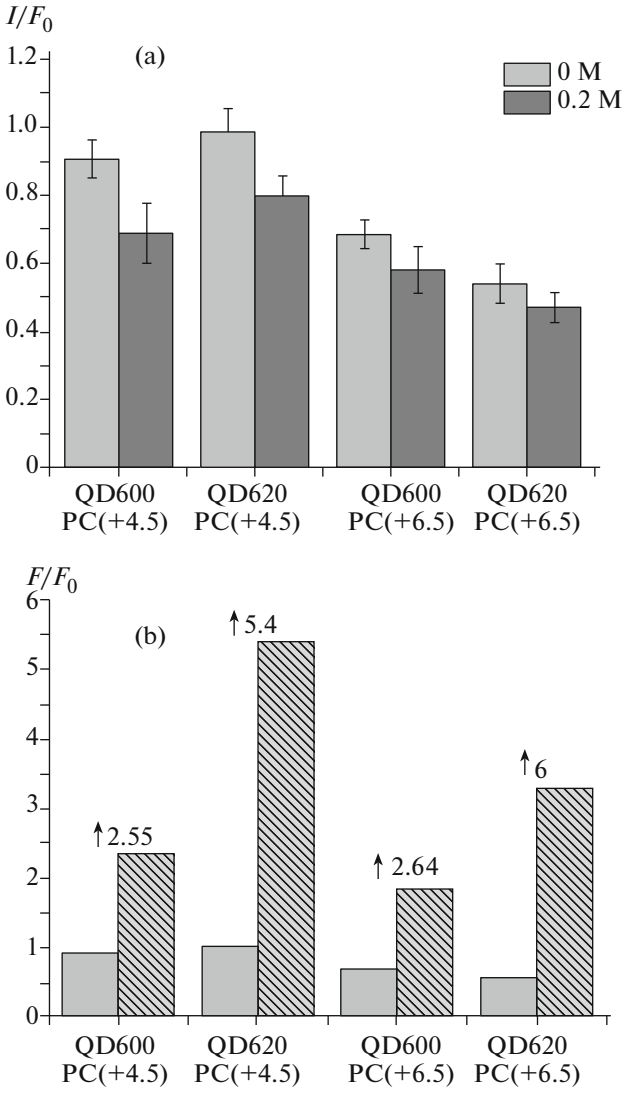

Fig. 5. (a) Fluorescence intensity of PCs I, assigned to its value F_0 in PC solution without QDs in pairs with different QDs upon ionic strength value to be 0 M (light grey bars) and 0.2 M (dark grey bars). Excitation wavelength is 655 nm. (b) Comparative changes in fluorescence intensity of PCs because of the hybrid complex formation (light grey bars from Fig. 5a) and as a result of energy migration (grey bars with lines). The data were taken from Table 4 for aqueous solution, $F/F_0 = A + 1$. The numbers with arrows indicate how many times fluorescence intensity of PC, located on QD surface, has been increased as a result of energy migration. [PC]/[QD] = 1 : 1.

100 : 1). When the PC concentration increases, parameter A reduces; in addition, the fluorescence enhancement coefficient becomes negative upon high PC concentrations, which confirms our assumptions. In this case, all the PC molecules are bound with QDs even at very high [PC]/[QD] ratios, because PC fluorescence enhancement coefficient remains still negative and kinetics of PC fluorescence anisotropy is described with a single-exponential approximation, which means that there are no free PC molecules in the solution. Indeed, an assessment of the surface area for QDs (about 210 nm^2 for QD600 and 410 nm^2 for QD620) suggests that there is a monolayer adsorption with a close packing of about 65 and 130 PC molecules, respectively (the PC molecule area in the macrocycle plane is about 3.2 nm^2). In fact, a greater number of PC molecules can adsorb on a QD surface; not all choline radicals may interact with charges of QD organic shell, i.e., when the plane of the PC molecule is perpendicular to the QD surface.

The kinetics of PC fluorescence anisotropy (Fig. 6b) differs by amplitude r_0, which reduces with an increase in the [PC]/[QD] ratio. The energy transfer is known to decrease fundamental anisotropy [34]. We assume that when local concentration of PC molecules rises on the QD surface, the probability of energy transfer between neighboring PC molecules

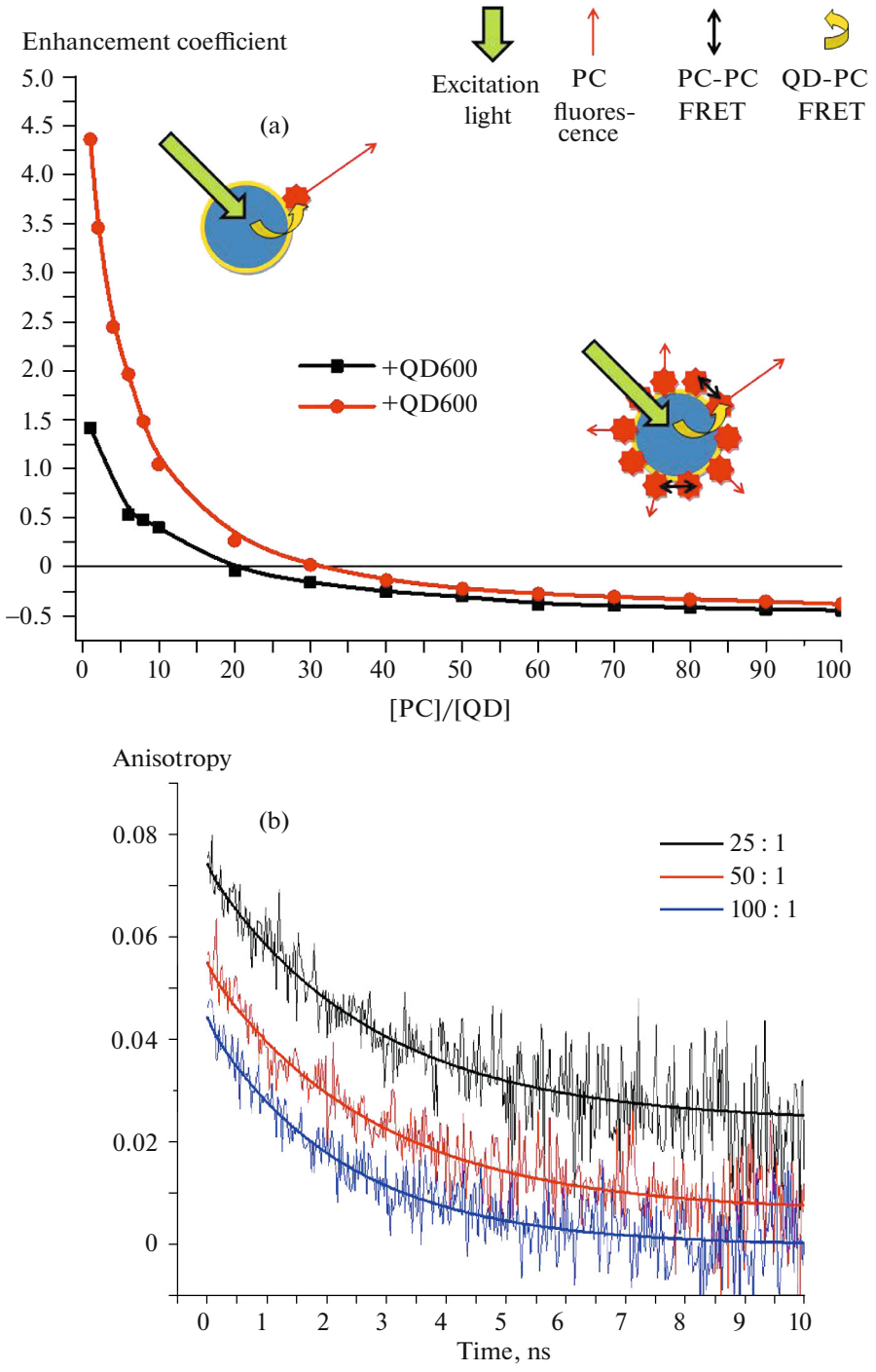

Fig. 6. (Color online) (a) Concentration dependence of fluorescence enhancement coefficient of PC(+4.5) in pairs with different QDs in aqueous solution and (b) kinetics of fluorescence anisotropy for PC(+4.5) in pair with QD600 at different [PC]/[QD] ratios. Incubation occurred within a half an hour.

increases (Förster mechanism [40]). The energy transfer can take place, because Stokes shift value in the PC spectrum is quite small to provide a significant overlap of the fluorescence spectra of the PC donor molecule and absorption spectrum of the PC acceptor one. It should be noted that in the control without QDs, the

relationship between PC fluorescence and its concentration appeared to be nonlinear to reach saturation and then become less with an increase in PC concentration more than 14 μM, which corresponds to [PC]/[QD] = 70 : 1 (Fig. 6a). The concentration quenching of PC fluorescence on the QD surface can probably occur upon even lower PC concentrations, which will cause a decrease in the PC enhancement coefficient to be measured.

CONCLUSIONS

In this work we studied the influence of ionic strength on stability and energy migration processes in hybrid complexes based on semiconductor quantum dots and substituted aluminum phthalocyanines. We have shown that electrostatic interaction in the QD/PC hybrid complex is sufficiently large, because an increase in ionic strength of the solution up to physiological values (0.15–0.2 M) does not disturb the stability of the QD/PC complex; moreover, NaCl ions in the solution enhance the efficiency of energy migration in the complex. Nevertheless, the behavior of the QD/PC complex in the internal environment of an organism requires further studies. Thus, the influence of many types of organic and inorganic ions, as well as protein fraction on properties of hybrid complexes are still weakly studied.

There is a decrease in phthalocyanine fluorescence intensity upon the formation of the complex with QDs without energy migration; this effect is defined by both the size of the QD and the number of positive charges on the periphery of the PC macrocycle molecule. This is possible only when a PC molecule interacts with a QD surface by its all side-chain substituents or at least a majority of them. This is confirmed by an experiment on studying the fluorescence anisotropy kinetics, when we did not observe an inherent rotation of PCs on the QD surface upon the formation of the hybrid complex in the solution. The decrease in PC fluorescence intensity is probably associated with a change in conformational state of the PC molecule adsorbed on the QD surface. Considering that the nature of the change in PC conformational state is determined by the force of electrostatic attraction to the quantum dot, an increase in ionic strength leads to a weakening of the electrostatic interaction and partial recovery of PC fluorescence intensity.

The relationships between the value of energy migration and qualitative and quantitative composition of the QD/PC complexes contribute significantly to the creation of hybrid complexes with improved photophysical and photochemical properties. According to our data, the use of quantum dots as artificial antenna complexes for PC molecules is only justified when the number of molecules of the energy acceptor per molecule of energy donor (QD) does not exceed 10–15. A further increase in the number of PC molecules leads to a significant decrease in its fluorescence intensity because of concentration quenching and in the inability of QDs to serve a large number of energy acceptors. The extremely low [PC]/[QD] ratios (1 : 1) are also disadvantageous because the energy migration efficiency in the hybrid complex is about 20%.

ACKNOWLEDGMENTS

This work was supported by the Russian Foundation for Basic Research (projects 15-04-01930 A, 15-29-01167 ofi_m, and 14-04-01536 A), the Russian Ministry of Education and Science (Grant from the Russian President no. MK-5949.2015.4), and the combined financial support of the Russian Foundation for Basic Research and Moscow Government (project 15-34-70007 mol_a_mos).

REFERENCES

1. J. D. Spikes, "Phthalocyanines as photosensitizers in biological systems and for the photodynamic therapy of tumors," Photochem. Photobiol. **43**, 691–699 (1986).
2. F. Lv, B. Cao, Y. Cui, and T. Liu, "Zinc phthalocyanine labelled polyethylene glycol: preparation, characterization, interaction with bovine serum albumin and near infrared fluorescence imaging in vivo," Molecules **17**, 6348–6361 (2012).
3. R. Bonnett, "Photosensitizers of the porphyrin and phthalocyanine series for photodynamic therapy," Chem. Soc. Rev. **24**, 19–33 (1995).
4. M. G. Strakhovskaya, Yu. N. Antonenko, A. A. Pashkovskaya, E. A. Kotova, V. Kireev, V. G. Zhukhovitsky, N. A. Kuznetsova, O. A. Yuzhakova, V. M. Negrimovsky, and A. B. Rubin, "Electrostatic binding of substituted metal phthalocyanines to enterobacterial cells: its role in photodynamic inactivation," Biochemistry (Moscow) **74**, 1305 (2009).
5. P. K. Selbo, A. Hogset, L. Prasmickaite, and K. Berg, "Photochemical internalisation: a novel drug delivery system," Tumour Biol. **23**, 103–112 (2002).
6. H. Ali and J. E. van Lier, "Metal complexes as photo- and radiosensitizers," Chem. Rev. **99**, 2379–2450 (1999).
7. D. A. Makarov, N. A. Kuznetsova, O. A. Yuzhakova, L. P. Savina, O. L. Kaliya, E. A. Luk'yanets, V. M. Negrimovskii, and M. G. Strakhovskaya, "Effects of the degree of substitution on the physicochemical properties and photodynamic activity of zinc and aluminum phthalocyanine polycations," Russ. J. Phys. Chem. A **83**, 1044 (2009).
8. T. Slastnikova, A. Rosenkranz, M. Zalutsky, and A. Sobolev, "Modular nanotransporters for targeted intracellular delivery of drugs: folate receptors as potential targets," Curr. Pharmaceut. Des. **21**, 1227–1238 (2009).
9. L. A. Muehlmann, B. C. Ma, J. P. Longo, M. de F. Almeida Santos, and R. B. Azevedo, "Aluminum-phthalocyanine chloride associated to poly(methyl vinyl ether-co-maleic anhydride) nanoparticles as a new third-generation photosensitizer for anticancer photodynamic therapy," Int. J. Nanomed. **9**, 1199–1213 (2014).
10. Y. Y. Huang, S. K. Sharma, R. Yin, T. Agrawal, L. Y. Chiang, and M. R. Hamblin, "Functionalized fullerenes in photodynamic therapy," J. Biomed. Nanotechnol. **10**, 1918–1936 (2014).

11. D. A. Tekdas, M. Durmus, H. Yanıka, and V. Ahsena, "Photodynamic therapy potential of thiol-stabilized CdTe quantum dot-group 3A phthalocyanine conjugates (QD-Pc)," Spectrochim. Acta, Part A **93**, 313–320 (2012).
12. A. Skripka, J. Valanciunaite, G. Dauderis, V. Poderys, R. Kubiliute, and R. Rotomskisa, "Two-photon excited quantum dots as energy donors for photosensitizer chlorin e6," J. Biomed. Opt. **18**, 078002 (2013).
13. L. Li, J. F. Zhao, N. Won, H. Jin, S. Kim, and J. Y. Chen, "Quantum dot aluminum phthalocyanine conjugates perform photodynamic reactions to kill cancer cells via fluorescence resonance energy transfer (FRET)," Nanoscale Res. Lett. **7**, 386 (2012).
14. O. S. Viana, M. S. Ribeiro, A. C. Rodas, J. S. Reboucas, A. Fontes, and B. S. Santos, "Comparative study on the efficiency of the photodynamic inactivation of candida albicans using CdTe quantum dots, Zn(II) porphyrin and their conjugates as photosensitizers," Molecules **20**, 8893–8912 (2015).
15. S. D'Souza, E. Antunes, and T. Nyokong, "Synthesis and photophysical studies of cdTe quantum dot-monosubstituted zinc phthalocyanine conjugates," Inorg. Chim. Acta **367**, 173–181 (2011).
16. A. C. S. Samia, X. Chen, and C. Burda, "Semiconductor quantum dots for photodynamic therapy," J. Am. Chem. Soc. **125**, 15736–15737 (2003).
17. S. B. Rizvi, S. Rouhi, S. Taniguchi, S. Y. Yang, M. Green, M. Keshtgar, and A. M. Seifalian, "Near-infrared quantum dots for HER2 localization and imaging of cancer cells," Int. J. Nanomed. **9**, 1323–1237 (2014).
18. S. Kamila, C. McEwan, D. Costley, J. Atchison, Y. Sheng, G. R. Hamilton, C. Fowley, and J. F. Callan, "Diagnostic and therapeutic applications of quantum dots in nanomedicine," Top. Curr. Chem. **370**, 203–224 (2016).
19. V. Biju, S. Mundayoor, R. V. Omkumar, A. Anas, and M. Ishikawa, "Bioconjugated quantum dots for cancer research: present status, prospects and remaining issues," Biotechnol. Adv. **28**, 199–213 (2010).
20. H. Hafian, A. Sukhanova, M. Turini, P. Chames, D. Baty, M. Pluot, J. H. Cohen, I. Nabiev, and J. M. Millot, "Multiphoton imaging of tumor biomarkers with conjugates of single-domain antibodies and quantum dots," Nanomedicine **10**, 1701–1709 (2014).
21. B. R. Liu, H. H. Chen, M. H. Chan, Y. W. Huang, R. S. Aronstam, and H. J. Lee, "Three arginine-rich cell-penetrating peptides facilitate cellular internalization of red-emitting quantum dots," J. Nanosci. Nanotechnol. **15**, 2067–2078 (2015).
22. A. A. Karpulevich, E. G. Maksimov, N. N. Sluchanko, A. N. Vasiliev, and V. Z. Paschenko, "Highly efficient energy transfer from quantum dot to allophycocyanin in hybrid structures," J. Photochem. Photobiol. B: Biol. **160**, 96–101 (2016).
23. F. J. Schmitt, E. G. Maksimov, P. Hätti, J. Weißenborn, V. Jeyasangar, A. P. Razjivin, V. Z. Paschenko, and G. Renger, "Coupling of different isolated photosynthetic light harvesting complexes and CdSe/ZnS nanocrystals via Förster resonance energy transfer," Biochim. Biophys. Acta, Bioenerg. **1817**, 1461–1470 (2012).
24. T. Nyokong and E. Antunes, "Photochemical and photophysical properties of metallophthalocyanines," in *Handbook of Porphyrin Science,* Ed. by K. M. Kadish, K. M. Smith, and R. Guilard (World Scientific, Singapore, 2010), **Vol. 7**, pp. 247–357.
25. E. G. Maksimov, D. A. Gvozdev, M. G. Strakhovskaya, and V. Z. Pashchenko, "Hybrid structures of polycationic aluminum phthalocyanines and quantum dots," Biochemistry (Moscow) **80**, 323 (2015).
26. W. W. Yu, L. Qu, W. Guo, and X. Peng, "Experimental determination of the extinction coefficient of CdTe, CdSe, and CdS nanocrystals," Chem. Mater. **15**, 2854–2860 (2003).
27. R. F. Kubin and A. N. Fletcher, "Fluorescence quantum yields of some rhodamine dyes," J. Lumin. **27**, 455–462 (1982).
28. I. E. Borissevitch, "More about the inner filter effect: corrections of Stern-Volmer fluorescence quenching constants are necessary at very low optical absorption of the quencher," J. Lumin. **81**, 219–224 (1999).
29. PML'16'C, *16 Channel Detector Head for Timecorrelated Single Photon Counting,* User Handbook (Becker and Hickl, Berlin, 2006). http://www.becker_hickl.de/pdf/pml16c21.pdf.
30. L. P. Aggarwal and I. E. Borissevitch, "On the dynamics of the TPP4 aggregation in aqueous solutions: successive formation of H and J aggregates," Spectrochim. Acta A: Mol. Biomol. Spectrosc. **63**, 227–233 (2006).
31. H. L. Ma and W. J. Jin, "Studies on the effects of metal ions and counter anions on the aggregate behaviors of meso-tetrakis(p-sulfonatophenyl)porphyrin by absorption and fluorescence spectroscopy," Spectrochim. Acta A: Mol. Biomol. Spectrosc. **71**, 153–160 (2008).
32. A. Cordones and S. Leone, "Mechanisms for charge trapping in single semiconductor nanocrystals probed by fluorescence blinking," Chem. Soc. Rev. **42**, 3209–3221 (2013).
33. M. Grabolle, J. Ziegler, A. Merkulov, T. Nann, and U. Resch-Genger, "Stability and fluorescence quantum yield of CdSe–ZnS quantum dots-influence of the thickness of the ZnS shell," Ann. N. Y. Acad. Sci. **1130**, 235–241 (2008).
34. J. R. Lakowicz, *Principles of Fluorescence Spectroscopy,* 3rd ed. (Springer, New York, 2006).
35. T. Tao, "Time-dependent fluorescence depolarization and brownian rotational diffusion coefficients of macromolecules," Biopolymers **8**, 609–632 (1969).
36. K. Kadish and R. Guilard, *The Porphyrin Handbook,* Vol. 17: *Phthalocyanines Properties and Materials* (Academic, New Yor, 2002).
37. J. M. Tsay, M. Trzoss, L. Shi, X. Kong, M. Selke, M. E. Jung, and S. Weiss, "Singlet oxygen production by peptide-coated quantum dot-photosensitizer conjugates," J. Am. Chem. Soc. **129**, 6865–6871 (2007).
38. A. Rakovich, T. Rakovich, V. Kelly, V. Lesnyak, A. Eychmuller, Y. P. Rakovich, and J. F. Donegan, "Photosensitizer methylene blue-semiconductor nanocrystals hybrid system for photodynamic therapy," J. Nanosci. Nanotechnol. **10**, 2656–2662 (2010).
39. X. Zhang, Z. Liu, L. Ma, M. Hossu, and W. Chen, "Interaction of porphyrins with cdTe quantum dots," Nanotechnology **22**, 195501 (2011).
40. Z. Petrásek and D. Phillips, "A time-resolved study of concentration quenching of disulfonated aluminium phthalocyanine fluorescence," Photochem. Photobiol. Sci. **2**, 236–244 (2003).

Translated by A. Tulyabaev